

Size and structural dependence of the magnetic properties of small 3d-transition-metal clusters

G. M. Pastor, J. Dorantes-Dávila,* and K. H. Bennemann

*Institut für Theoretische Physik, Freie Universität Berlin, Arnimallee 14,
D-1000 Berlin 33, Federal Republic of Germany*

(Received 17 February 1989; revised manuscript received 16 August 1989)

The size and structural dependence of magnetic properties of small Cr_n , Fe_n , and Ni_n clusters are determined by using a tight-binding Hubbard Hamiltonian in the unrestricted Hartree-Fock approximation. Results are given for the average magnetic moment $\bar{\mu}_n$, local magnetic moments, and magnetic ordering at $T=0$. We obtain for Fe_n ($n \leq 15$) that $\bar{\mu}_n$ varies as a function of n due to the interplay between the changes in coordination number and bond length as a function of cluster size, which may be related to recent experiments. The dependence of the structural cluster stability on magnetism is discussed. Results are also given for the cohesive energy, average bond length, and local densities of states.

I. INTRODUCTION

In the past, small metal clusters were mainly used as models for calculating surface or bulk electronic properties. However, in the last few years considerable interest in the properties of clusters themselves has developed, due to the possibility of studying them experimentally and their increasing importance in technological applications.¹

One of the fundamental problems in cluster research is to understand how the physical properties change as the electrons of a single atom become part of a group of several atoms and delocalize, and how bulklike behavior is achieved. Particularly interesting in this respect are the magnetic properties of transition-metal clusters. The magnetism of bulk-transition metals is namely known to be due to itinerant d electrons on the metallic side in contrast to the magnetism of atoms and insulators which is due to electrons localized in atomiclike orbitals. Thus, the study of this problem will also help to answer the fundamental question of electron delocalization as a function of cluster size. Furthermore, interesting structural dependence of the magnetic properties of transition metals has been observed, which reflects the sensitivity of these to the details in the electronic structure. For example, bcc α -Fe is ferromagnetic with a magnetic moment $\mu_b = 2.21\mu_B$ at $T=0$, whereas fcc γ -Fe seems to be weakly antiferromagnetic ($\mu_b = 0.7\mu_B$).^{2,3} The magnetization is also very sensitive to changes in the local environment that occur at surfaces, alloys, or by applying external pressure.⁴⁻⁶ Since in a small cluster the local environment (e.g., coordination number) and structure vary sensitively with cluster size n , one expects transition-metal clusters to show a wide variety of magnetic phenomena as a function of n .

Recently, Cox *et al.*⁷ performed for the first time magnetic deflection experiments on free Fe clusters. They observed that the average magnetic moment per atom $\bar{\mu}_n$ of Fe_n ($n \leq 17$) is larger than or equal to that of the bulk. Concerning the size dependence of $\bar{\mu}_n$ they concluded that $\bar{\mu}_n$ should be constant or could even increase with

increasing cluster size. Variations of $\bar{\mu}_n$ as a function of n can be inferred,⁷ possibly somewhat speculative.

So far, most of the theoretical studies on the magnetic properties of transition-metal clusters were performed using first-principle methods.⁸⁻¹³ These type of calculations do provide the highest precision and reliability one can reach nowadays, but require a great deal of computational effort. Thus, they are limited to small clusters ($n \lesssim 15$) with high symmetry. In agreement with experiment⁷ one obtains⁸⁻¹⁰ for Fe_n and Cr_n ($n=9,15$) larger magnetic moments than for the bulk. However, very little can be said about the cluster-size dependence of $\bar{\mu}_n$, the role of cluster relaxation (i.e., geometry optimization), or finite-temperature effects [e.g., transition temperature $T_c(n)$]. In this paper we report results of calculations of several properties of transition-metal clusters: size dependence of $\bar{\mu}_n$, local magnetic moments (i.e., magnetic ordering), cohesive energy, average bond length, and local densities of states. These were obtained using a tight-binding Hubbard Hamiltonian^{14,15} in the unrestricted Hartree-Fock approximation. This method, which we describe in Sec. II, has been applied successfully to bulk¹⁶ and surfaces^{4,5} and is expected to provide valuable complementary information to first-principles calculations.

In Sec. III we present and discuss our results in some detail. We obtain for $\bar{\mu}_n$ reasonable agreement with previous calculations⁸⁻¹⁰ performed for unrelaxed clusters (i.e., using bulk bond length). However, by allowing cluster relaxation the clusters contract in order to minimize the total energy. This causes important changes in $\bar{\mu}_n$ ($n \lesssim 15$) which improve qualitatively the agreement with the observed⁷ size dependence of $\bar{\mu}_n$ for Fe_n . In Sec. IV a summary of the conclusions is given. Preliminary results of some of the calculations have already been reported previously.^{14,15}

II. THEORY

In order to study the size and structural dependence of the magnetic properties we consider the Hubbard Hamil-

tonian for d electrons which are expected to contribute dominantly,¹⁷

$$H = \sum_{\substack{i \neq j \\ \alpha, \beta, \sigma}} t_{ij}^{\alpha\beta} c_{i\alpha\sigma}^\dagger c_{j\beta\sigma} + H_I, \quad (1)$$

where $c_{i\alpha\sigma}^\dagger$ ($c_{i\alpha\sigma}$) refers to the creation (annihilation) operator of an electron with spin σ at atomic site i in the orbital α ($\alpha = xy, yz, zx, x^2 - y^2, 3z^2 - r^2$) and $t_{ij}^{\alpha\beta}$ to the hopping integrals for d electrons between sites i and j . The interaction Hamiltonian H_I in the unrestricted Hartree-Fock approximation is given by

$$H_I = \sum_{i, \sigma} \varepsilon_{i\sigma} \hat{n}_{i\sigma} - E_{dc}, \quad (2)$$

$$\varepsilon_{i\sigma} = \varepsilon_d^0 + U \Delta n(i) - \frac{1}{2} \sigma J \mu(i).$$

Here, $\hat{n}_{i\sigma}$ refers to the d -electron number operator and $E_{dc} = \frac{1}{2} \sum_{i, \sigma} (\varepsilon_{i\sigma} - \varepsilon_d^0) \langle n_{i\sigma} \rangle$ to the correction due to double counting. The exchange and effective direct intra-atomic Coulomb integrals, denoted by J and U , respectively, are taken to be independent of cluster size and are given by $J = (U_{\uparrow\downarrow} - U_{\uparrow\uparrow})$, $U = (U_{\uparrow\downarrow} + U_{\uparrow\uparrow})/2$, where $U_{\uparrow\downarrow}$ and $U_{\uparrow\uparrow}$ are the Coulomb interaction between electrons with opposite and parallel spin including exchange, respectively. The number of d electrons $n(i)$ and the local magnetic moment $\mu(i)$ at site i given by

$$\mu(i) = \langle \hat{n}_{i\uparrow} \rangle - \langle \hat{n}_{i\downarrow} \rangle, \quad (3)$$

$$n(i) = \langle \hat{n}_{i\uparrow} \rangle + \langle \hat{n}_{i\downarrow} \rangle,$$

are determined self-consistently by requiring

$$\langle n_{i\sigma} \rangle = \int_{-\infty}^{\varepsilon_F} N_{i\sigma}(\varepsilon) d\varepsilon. \quad (4)$$

Note that we allow charge transfer between different atomic sites i by requiring global charge neutrality: $\Delta n(i) = n(i) - n_d$, $n_d = (1/n) \sum_i n(i)$. The spin-polarized local densities of states (DOS) $N_{i\sigma}(\varepsilon)$ are calculated by using the Haydock-Heine-Kelly recursion method.¹⁸ We assume for the hopping integrals the canonical values^{19,20} varying as the inverse fifth power of the interatomic distance d : $(dd\sigma) = -6(W_d/2.5)(r_{WS}/d)^5$, $(dd\pi) = 4(W_d/2.5)(r_{WS}/d)^5$, and $(dd\delta) = -1(W_d/2.5)(r_{WS}/d)^5$. Here, W_d stands for the bulk d -band width and r_{WS} for the Wigner-Seitz radius. For bcc- and icosahedral-like structures, we take into account nearest- and next-nearest-neighbor hopping integrals, while for fcc-like structures only nearest-neighbor hopping integrals are included. Note that the cluster magnetic order (e.g., ferromagneticlike or antiferromagneticlike) is given by the sign of $\mu(i)$. The average magnetic moment $\bar{\mu}_n$ given by

$$\bar{\mu}_n = \frac{1}{n} \sum_{i=1}^n \mu(i) \quad (5)$$

represents the average magnetization of the cluster at $T=0$. Although we have restricted here to properties at $T=0$, the theory can be extended to finite temperatures within the functional-integral formalism¹⁶ or the alloy-analogy model,²¹ for example.

The cohesive energy per cluster atom is given by

$$E_{\text{coh}}(n) = E_{\text{band}}(1) - E_{\text{band}}(n) - E_R, \quad (6)$$

where $E_{\text{band}}(n)$ refers to the electronic d -band contribution per atom,

$$E_{\text{band}}(n) = \frac{1}{n} \sum_{i=1}^n \int_{-\infty}^{\varepsilon_F} \varepsilon N_{i\sigma}(\varepsilon) d\varepsilon - E_{dc}. \quad (7)$$

The Born-Meyer repulsive energy E_R is calculated from

$$E_R = \frac{1}{2n} \sum_{i=1}^n z_i A \exp \left[-p \left(\frac{d}{d_b} - 1 \right) \right], \quad (8)$$

where z_i refers to the coordination number at site i and d_b to the bulk interatomic distance. The parameters A and p are fitted to the bulk equilibrium condition and compressibility modulus. We allow uniform relaxation, then we minimize the energy with respect to d and obtain the average equilibrium bond length d_n , the cohesive energy $E_{\text{coh}}(n)$, and the magnetic moments for each assumed structure. Note that in calculating the cluster-size dependence of the magnetic properties and cohesive energy, we neglect for simplicity the s -electron contribution and s - d hybridization effects, but the model could be easily extended to take them self-consistently into account. As discussed below, s electrons and s - d hybridization effects seem not to contribute much to the size and structural dependence of the magnetic properties we calculate. However in some cases, s electrons can be important for determining bond-length or structural changes on which, as will be shown, the magnetic properties do depend.

III. RESULTS AND DISCUSSION

Using the theory outlined in Sec. II we determine the size dependence of the average magnetic moment $\bar{\mu}_n$, magnetic moments $\mu(i)$ at site i (i.e., magnetic ordering), cohesive energy $E_{\text{coh}}(n)$, and equilibrium interatomic distance d_n of small Cr_n , Fe_n , and Ni_n clusters. The parameters used for the calculations are listed in Table I. n_d is taken to be independent of size²² and such that the number of s electrons $n_s = 1$. J is fitted to the bulk magnetic moment μ_b , W_d is taken from band calculations,²³ and U is estimated from atomic-spectroscopic data.^{24,25} In practice this is almost equivalent to the limit $U \rightarrow \infty$ and implies approximately local charge neutrality. In previous calculations for Fe clusters¹⁵ we showed that the magnetic properties are not very sensitive to the value of

TABLE I. Parameters used for the calculations (see text). n_d refers to the number of electrons per atom.

n_d	W_d (eV)	J (eV)	U (eV)	μ_b (μ_B)	
Cr	5.0	7.0	0.56	6.3	0.60
Fe	7.0	6.0	0.73	5.4	2.21
Ni	9.0	5.0	0.50	4.5	0.60

U since $\Delta n(i)$ is small even for $U=0$. For small clusters ($n < 9$) we assume the various probable structures shown in Tables II–V and for larger clusters bcc-, fcc-, or icosahedral-like structures obtained by adding to a central atom the successive shells of its first, second, etc., neighbors (see Fig. 1).

Concerning the accuracy of the continued fraction expansion¹⁸ of the local Green's functions G_{ii} we would like to point out that for small clusters ($n \lesssim 8$) the off-diagonal recursion coefficient b_N vanishes for $N \approx 6-10$, implying that the recursive expansion is equivalent to numerical diagonalization. For larger clusters ($n \gtrsim 15$) we take N large enough such that the results become independent of N . Empirically, we found that $N \approx 25-40$ satisfies this condition. To avoid oscillations in the numerical solution of the self-consistent equations (2)–(4) the discrete cluster energy levels were first broadened by calculating the Green's functions $G(z)$ at an imaginary energy $z = \epsilon + i\gamma$. In successive iterations we then let $\gamma \rightarrow 0$ and obtain the self-consistent magnetic moments for the proper discrete energy spectrum of the cluster.

For all studied clusters we obtain larger magnetic moments than for bulk material. This can be understood recalling that in a small cluster most of the atoms have a smaller coordination number and therefore the effective d -band-width $W_d(n)$ is smaller than in bulk material. Thus, the kinetic-energy loss upon magnetization is smaller [$\Delta E_{\text{kin}} \propto 1/N(\epsilon) \propto W_d(n)$] yielding larger local magnetic moments. For the same reason $\mu(i)$ generally increases for Cr_n and Fe_n ($n \geq 9$) as we go from the center to the surface of the cluster [$\mu(1) < \mu(2) < \mu(3)$], i.e., as the local coordination number decreases (see Tables III

and IV). Similar behavior has been observed at surfaces of transition metals.^{4,5} Note that the increase of $\mu(i)$ becomes more and more important as we go from Ni to Cr, i.e., as we approach half-band-filling, since more holes are available to be polarized, and that unrelaxed Cr_n shows even larger local magnetic moments than Fe_n in contrast to bulk material. A similar large increase of $\mu(i)$ has also been obtained for Cr surfaces.⁴ For Ni clusters the local magnetic moments $\mu(i)$ decrease as we go from the center to the surface of the cluster. This results because charge is transferred from the inner atoms to the surface atoms which have a smaller effective bandwidth. The larger number of d holes allows namely a larger spin polarization of the inner atoms. Note that $\mu(1) > 1.0\mu_B$ can only be obtained if $n(1) < n_d = 9.0$ (see Table V).

A. Fe_n clusters

Results for very small clusters ($n \leq 8$) are given in Table II. Using the normal bulk bond length, we obtain saturated magnetic moments [$\mu(i) = [10 - n_d(i)]\mu_B \approx 3.0\mu_B$], i.e., fully polarized d band. The magnetic order within the cluster was found in all cases ($n \leq 8$) to be ferromagneticlike. Notice that the total magnetic moment $n\bar{\mu}_n$ of the cluster must be an integer multiple of μ_B , since the total spin operator $S = \sum_i (\hat{n}_{i\uparrow} - \hat{n}_{i\downarrow})$ commutes with H . However, small variations of $\mu(i)$ versus i are obtained due to the small charge transfer [$\Delta n_d(i) \sim 0.01$].

Allowing uniform relaxation the cluster bond length contracts in order to minimize the total energy. The value of the contraction varies from about 10% for the dimer and trimer, to 1–2% for the larger clusters with a more close-packed arrangement of the atoms. Since the magnetic moments are saturated in this size range ($n \leq 8$), no significant change of $\bar{\mu}_n$ is obtained upon contraction. This holds even for the dimer and linear trimer, for which a large reduction of the bond length is obtained. A remarkable exception is, however, provided by the triangular trimer. Here a 9% contraction causes the total magnetic moment $n\bar{\mu}_n$ to change from $9\mu_B$ to $7\mu_B$ ($\bar{\mu}_3 = 3\mu_B \rightarrow \bar{\mu}_3 = 2.33\mu_B$). This reduction occurs because the splitting of the molecular orbitals (effective d -bandwidth) increases with decreasing bond length ($W_d \sim d^{-5}$). As a consequence the highest occupied spin-up molecular orbital becomes unoccupied (lies above ϵ_F) after contraction and one more spin-down molecular orbital becomes occupied. The fractional value of $\bar{\mu}_3$ ($\bar{\mu}_3 = \frac{7}{3} \approx 2.33$) results from the fact that in our calculations the electrons occupy delocalized molecular orbitals. This might be a consequence of the Hartree-Fock approximation used for calculating $\mu(i)$, which in very small clusters might tend to overestimate the d -band width and thus might be not accurate for $n \leq 8$. An improved treatment of electron correlations possibly yields saturated local magnetic moments also for relaxed Fe_3 . Similarly, $\bar{\mu}_9$ changes from $3.0\mu_B$ to $2.33\mu_B$, since three majority spin levels move above ϵ_F after contraction ($\bar{\mu}_9 = \frac{27}{9} \rightarrow \bar{\mu}_9 = \frac{21}{9}$). This shows the strong sensitivity of the magnetic properties of $3d$

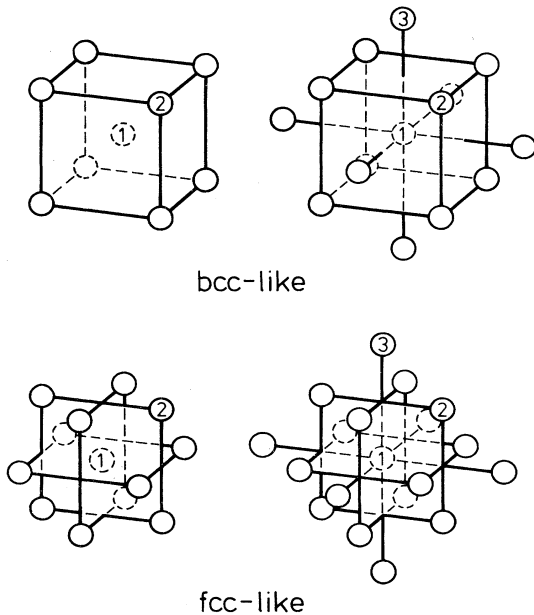


FIG. 1. Illustration of the bcc- and fcc-like cluster geometry. The different shells are labeled 1,2 etc.

TABLE II. Results for the size and structural dependence of the cohesive energy $E_{\text{coh}}(n)$ (in eV), average bond length d_n (d_b = bulk bond length), average magnetic moment $\bar{\mu}_n$, and local magnetic moments $\mu(i)$ (in units of μ_B), of small Fe_n clusters ($n \leq 8$). Different symmetry atoms i are indicated in the assumed geometries. Results for the unrelaxed geometries are given in parentheses.

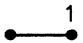

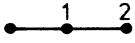

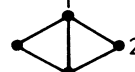

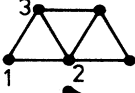




	Structure	$E_{\text{coh}}(n)$	d_n/d_b	$\bar{\mu}_n$	$\mu(1)$	$\mu(2)$	$\mu(3)$
Fe_2		0.92 (0.81)	0.90	3.00 (3.00)	3.00 (3.00)		
Fe_3		1.21 (1.12)	0.91	2.33 (3.00)	2.33 (3.00)		
Fe_3		0.80 (0.74)	0.94	3.00 (3.00)	2.98 (2.98)	3.01 (3.01)	
Fe_4		1.31 (1.26)	0.97	3.00 (3.00)	3.00 (3.00)		
Fe_4		1.32 (1.26)	0.96	3.00 (3.00)	2.98 (2.99)	3.02 (3.01)	
Fe_5		1.39 (1.37)	0.97	3.00 (3.00)	2.98 (2.99)	3.02 (3.02)	
Fe_5		1.29 (1.25)	0.96	3.00 (3.00)	3.03 (3.02)	2.98 (2.99)	2.98 (2.99)
Fe_6		1.26 (1.23)	0.99	3.00 (3.00)	3.01 (3.01)	2.97 (2.97)	
Fe_7		1.50 (1.49)	0.99	3.00 (3.00)	3.00 (3.00)	2.99 (3.00)	
Fe_8		1.42 (1.41)	0.99	3.00 (3.00)	3.00 (3.00)		
Fe_8		1.16 (1.14)	0.98	3.00 (3.00)	3.00 (3.00)		

TABLE III. Results as in Table II for larger Fe_n clusters ($n > 9$). Different shells i are indicated as in Fig. 1.

	Structure	$E_{\text{coh}}(n)$	d_n/d_b	$\bar{\mu}_n$	$\mu(1)$	$\mu(2)$	$\mu(3)$	$\mu(4)$	$\mu(5)$
Fe_9	bcc	1.37 (1.08)	0.91	2.33 (3.00)	0.40 (2.96)	2.57 (3.01)			
Fe_{11}	bcc	1.41 (1.36)	0.97	3.00 (3.00)	2.96 (2.96)	3.02 (3.02)	2.96 (2.97)		
Fe_{13}	bcc	1.62 (1.55)	0.97	2.54 (3.00)	0.42 (2.95)	2.65 (3.01)	2.85 (2.98)		
Fe_{13}	fcc	1.42 (1.41)	0.98	1.92 (2.08)	-1.71 (-1.79)	2.23 (2.40)			
Fe_{13}	icos.	1.41 (1.39)	0.98	2.08 (2.23)	-1.98 (-2.20)	2.41 (2.60)			
Fe_{15}	bcc	1.63 (1.60)	0.97	2.60 (2.73)	0.48 (1.28)	2.67 (2.88)	2.86 (2.76)		
Fe_{19}	fcc	1.42 (1.41)	0.99	1.84 (1.95)	-1.09 (-1.28)	1.76 (1.91)	2.49 (2.56)		
Fe_{27}	bcc	(1.41)		(2.85)	(2.88)	(2.67)	(2.85)	(2.97)	
Fe_{43}	fcc	(1.70)		(1.23)	(-1.37)	(-0.90)	(0.89)	(2.49)	
Fe_{51}	bcc	(1.73)		(2.45)	(1.28)	(1.87)	(1.57)	(2.62)	(2.83)
bulk	bcc	2.0	1.0	2.21	2.21				

transition metals to cluster size and structure.

For the difference in the cohesive energy $E_{\text{coh}}(n)$ between different assumed structures we obtain $\Delta E_{\text{coh}} \approx 0.01-0.09$ eV ($n=3-5$). These values are too small to conclude safely, taking into account the approximations we made, about the most stable geometrical arrangement of the atoms at $T=0$, but rather indicate that a strong coupling between electronic and translational degrees of freedom can be expected at finite temperatures.

In Table III results are given for larger Fe_n clusters ($9 \leq n \leq 51$) with bcc-like structure (see Fig. 1). These

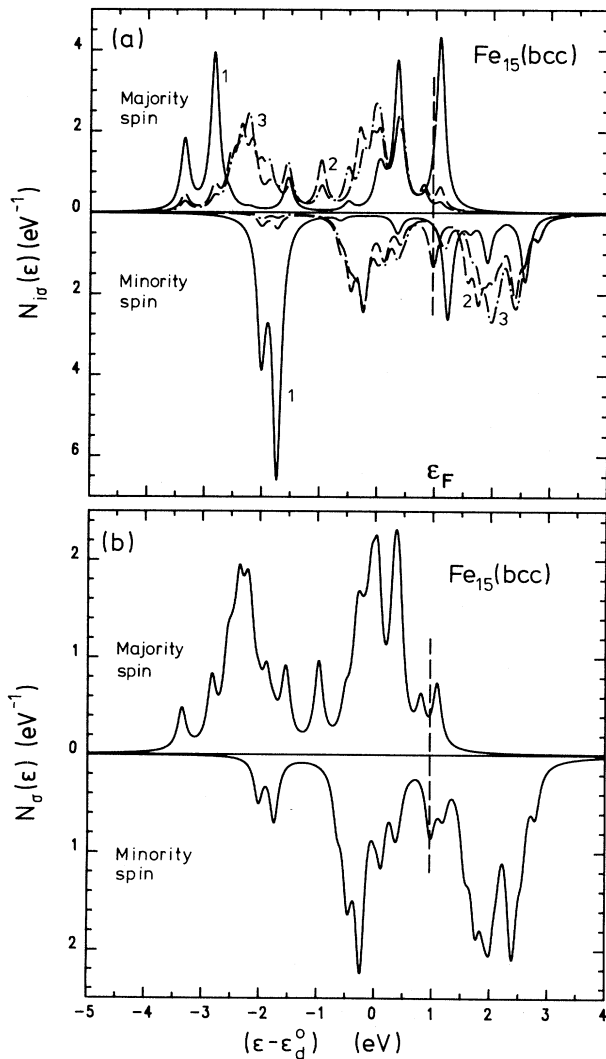


FIG. 2. (a) Local densities of states $N_{i\sigma}(\epsilon)$ of bcc- Fe_{15} . The numbers refer to different shells ordered by increasing distance to the cluster center as in Fig. 1. (b) Average density of states $N_{\sigma}(\epsilon) = (1/n) \sum_i N_{i\sigma}(\epsilon)$ of bcc- Fe_{15} . A Lorentzian was used to broaden the cluster energy levels ($\gamma=0.2$ eV).

clusters show in all cases ferromagneticlike order (i.e., all moments pointing in the same direction). Using the bulk bond length (results in parentheses) we obtain for $n \leq 13$ saturated local magnetic moments. Larger clusters ($n \geq 15$) have nonsaturated $\mu(i)$ [$\mu(i) < (10-n_d)\mu_B = 3.0\mu_B$] as the convergence towards bulklike behavior starts to take place. The local magnetic moments $\mu(i)$ show interesting environment dependence. For example, for unrelaxed Fe_{15} we obtain (in units of μ_B) $\mu(1)=1.28$, $\mu(2)=2.88$, and $\mu(3)=2.76$. The rather small value of $\mu(1)$ is due to the fact that the perturbation introduced by the cluster surface is symmetric around the central atom and therefore produces a very strong changes in its local DOS [see Fig. 2(a)]. Note that our results for $\mu(i)$ versus i are in good agreement with self-consistent-field- $X\alpha$ (SCF- $X\alpha$) calculations^{9,10} [$\mu_{X\alpha}(1)=0.9$, $\mu_{X\alpha}(2)=2.8$, and $\mu_{X\alpha}(3)=2.8$], suggesting that for Fe_n s electrons and s - d hybridization effects are not important for calculating $\mu(i)$ as noted for bulk calculations.¹⁷ Furthermore our result for the d -band width $W_d(n)$ of Fe_{15} [$W_d(15)=4.9$ eV] is close to that determined in local-spin-density-functional (LSDF) calculations⁸ [$W_d(15)=4.7-5.3$ eV]. This indicates, as physically expected, that the hopping integrals t_{ij} and Coulomb integrals U and J are approximately independent of cluster size, since these are local properties²⁶ and the shape of the rather localized d orbitals is not very environment dependent.²⁷

A more critical test²⁸ on the accuracy of our tight-binding calculations and the role of s - d hybridization is provided by the DOS of Fe_{15} shown²⁹ in Fig. 2. The shape of the total DOS indicates that a resemblance between the general features of the distribution of energy levels for the clusters and for the bulk starts to develop, as noted by the authors of Refs. 8 and 9. For example, the typical bonding and antibonding broad peaks of bcc bulk separated by a valley near the center of the band are already present. Due to the exchange splitting the energy of the antibonding up states is close to that of the bonding down states and the Fermi energy ϵ_F lies in the valley between these states and the antibonding down states. The d -level energy distribution agrees moderately well with first-principles calculations.^{8,9} The main discrepancy appears in the structure of the majority band. Here the energy difference we obtain between the two upper main peaks (~ 0.5 eV) is smaller than that obtained by Lee *et al.* (~ 1 eV). Note that the three-peaked structure obtained in LSDF calculations is a cluster feature not present in bulk Fe.³⁰ Although the total DOS of bcc Fe_{15} and of bulk Fe are quite similar one cannot conclude that this will be also the case for larger bcc-like clusters. For instance, the total DOS for Fe_{27} shown in Fig. 3(b) has new features which results from the contributions of the atoms in the outer shells of the cluster [see Fig. 3(a)]. This difference in the DOS for Fe_{15} and Fe_{27} can be qualitatively understood if one looks at the surface of both clusters. The bcc-like Fe_{15} cluster has a fairly closed surface while the surface of Fe_{27} is rather open. The effective bandwidth of the outermost atoms of Fe_{27} (labeled 4) is much smaller than that of the inner atoms.

New surfacelike states (extended mainly on shells 3 and 4) are present in Fe_{27} around 1 eV (-1.2 eV) for minority (majority) spin, which spoils the resemblance to the bulk total DOS (see Fig. 3). For similar reasons the local mag-

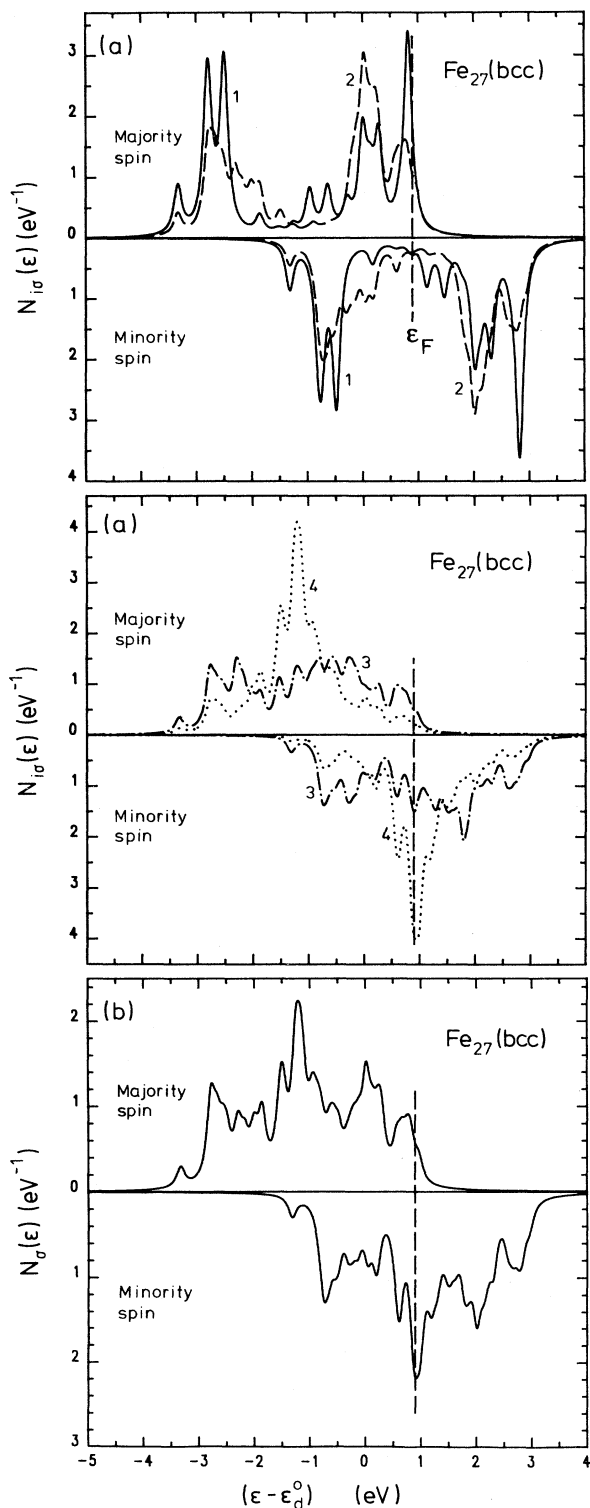


FIG. 3. (a) Local densities of states $N_{i\sigma}(\epsilon)$ and (b) average density of states $N_{\sigma}(\epsilon)$ of bcc- Fe_{27} as in Fig. 2.

netic moments $\mu(i)$ in bcc-like Fe_{51} have not yet converged to bulk values.³¹ The open surface of Fe_{27} and Fe_{51} also manifests in the rather low values of their cohesive energy. Therefore we expect the surface to reconstruct to a closer one possibly resembling that of Fe_{15} .

In Table III, results for fcc- and icosahedral-like Fe_n clusters are also given. These clusters show antiferromagneticlike ordering with the magnetic moments of the central atom pointing in the direction opposite to that of the outermost shells (Fe_{13} : $\uparrow\downarrow\uparrow$, Fe_{19} : $\uparrow\uparrow\downarrow\downarrow\uparrow$, and Fe_{43} : $\uparrow\uparrow\downarrow\downarrow\uparrow\uparrow$). Similar behavior seems to be observed for small γ -Fe particles³² and is probably related to the antiferromagnetic ordering observed in bulk γ -Fe^{2,3}. The absolute values of the magnetic moments are usually somewhat smaller for fcc- or icosahedral-like Fe_n than for bcc-like Fe_n . However the enhancement with respect to the magnetic moment of bulk γ -Fe is very large [$\mu(i) \approx 3\mu(\gamma\text{-Fe})$; $\mu(\gamma\text{-Fe}) = 0.7\mu_B$]. Note that in the fcc lattice no perfect nesting of two antiferromagnetic sublattices is possible, i.e., there is always some frustration. Thus, the choice of the sublattices is not obvious. For example, the magnetization could alternate signs along the (001) direction as observed² for bulk γ -Fe. Therefore, more general calculations with no rotational symmetry restrictions are necessary to determine precisely the antiferromagnetic structure of fcc-like Fe_n .

Concerning the structural stability we obtain the bcc-like Fe_n clusters are more stable than fcc-like clusters for $n = 13-19$, in agreement with previous results³³ derived from the size dependence of the ionization energy of Fe clusters. This is due to the contribution of the magnetic energy gain $\Delta E_{\text{mag}}(n) = E_{\text{band}}(\mu=0) - E_{\text{band}}(\mu)$, which is much larger for bcc clusters [$\Delta E_{\text{mag}}^{\text{bcc}}(13) \approx 0.4$ eV] than for the fcc clusters [$\Delta E_{\text{mag}}^{\text{fcc}}(13) \approx 0.1$ eV]. This contribution overcomes the larger kinetic-energy gain of the fcc structure, which would be more stable if magnetic contributions were neglected [$E_{\text{coh}}^{\text{fcc}}(\mu=0) - E_{\text{coh}}^{\text{bcc}}(\mu=0) \approx 0.08$ eV]. For bulk Fe we obtain a similar behavior in accordance with previous calculations.³⁴

In Fig. 4 we show a plot for $\bar{\mu}_n$ as a function of cluster size. For each n the structure of largest $E_{\text{coh}}(n)$ shown in Tables II and III is used. For the unrelaxed clusters we find saturated magnetic moments ($n \leq 13$). As a result $\bar{\mu}_n$ exhibits a very weak dependence on the geometrical structure of the clusters in agreement with density-functional results.^{8,9} However for relaxed clusters we find that μ_n changes strongly for $n = 3, 9$ and $n = 13-15$. This shows that $\bar{\mu}_n$ may depend sensitively on the bond length d_n and cluster geometry. The dependence of $\bar{\mu}_n$ on d_n results from the fact that when d_n decreases the splitting of the molecular orbitals (effective d -band width) increases. As a result $\bar{\mu}_n$ decreases. For $n = 4-8$ we obtain for $\bar{\mu}_n$ the same results for relaxed and unrelaxed clusters, although the relaxation is about 4%, due to the fact that the $\mu(i)$ are saturated. For $n = 3$ and $n = 9$ our calculations yield such a strong relaxation ($\sim 9\%$) that this reduces $\bar{\mu}_n$, even so for the corresponding unrelaxed clusters the $\mu(i)$ are also saturated. For $n = 13-15$ we obtain large changes in $\bar{\mu}_n$, though the relaxation is relatively

small ($\sim 2-3\%$), since for these clusters the $\mu(i)$ are no longer saturated as is known to be the case for bulk Fe. Comparison with experimental results for $\bar{\mu}_n$ derived indirectly from the depletion factor D_n indicates discrepancies with our calculations, although the main trends are well reproduced particularly for $n > 9$. Notice that we obtain a rapid increase of $\bar{\mu}_n$ for $n=3 \rightarrow 4$ and then an almost constant $\bar{\mu}_n$ for $4 \leq n \leq 7$, instead of the experimentally observed smooth increase of $\bar{\mu}_n$ for $3 \leq n \leq 7$. This may result from uncertainties⁷ in the relation between $\bar{\mu}_n$ and D_n or also from our neglect of s electrons in determining cluster relaxation. s -electron contributions may favor contraction particularly for the smaller clusters and thus reduce $\bar{\mu}_n$. Similarly as interpreting $\bar{\mu}_3 = \frac{7}{3}\mu_B = 2.33\mu_B$ one may continue to argue as follows: For the small clusters, the bond-length decrease may cause the highest spin-up molecular orbital to move above the Fermi level. Thus, one may obtain $\bar{\mu}_4 = \frac{10}{4}\mu_B = 2.5\mu_B$, $\mu_5 = \frac{13}{5}\mu_B = 2.6\mu_B$, $\mu_6 = \frac{16}{6}\mu_B = 2.67\mu_B$, $\mu_7 = \frac{19}{7}\mu_B = 2.71\mu_B$, and $\mu_8 = \frac{22}{8}\mu_B = 2.75\mu_B$. It is interesting to see that in this way one obtains much better agreement with experimental results. Since our numerical calculations do underestimate bond-length contraction, the resulting increase of the splitting of the molecular orbitals may be too small to cause such a shift of a spin-up molecular orbital above ϵ_F . Note that we have neglected the repulsive interaction between second neighbors and thus our estimations of d_n might be quantitatively not correct for bcc clusters. Furthermore, cluster relaxation might not be of the simple form assumed here (uniform relaxation), which retains high symmetry.³⁵ This could influence the size dependence of $\bar{\mu}_n$, since the magnetic properties are sensitive to the cluster structure.

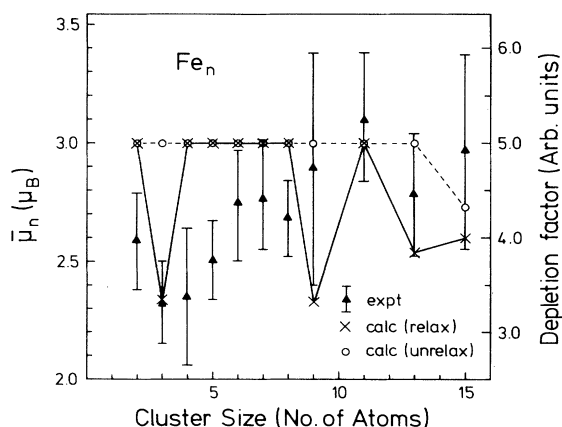


FIG. 4. Average magnetic moment $\bar{\mu}_n$ of Fe_n clusters as a function of n . Crosses (circles) refer to calculations for relaxed (unrelaxed) clusters. Experimental results for the depletion factor (approximately proportional to $\bar{\mu}_n$) are indicated by the vertical bars (Ref. 7).

In particular for Fe_9 , additional effects related to the expected³³ Jahn-Teller distortion could appear. For $n=2,3$ direct experimental determination of $\bar{\mu}_n$ yields⁷ $\bar{\mu}_2 = (3.3 \pm 0.5)\mu_B$, $\bar{\mu}_3 = (2.7 \pm 0.3)\mu_B$, while we obtain $\bar{\mu}_2 = 3.0\mu_B$ and $\bar{\mu}_3 = 2.33\mu_B$. Notice that for clusters with an odd number of atoms an additional contribution to the average magnetic moment $\bar{\mu}_n$ results at $T=0$ from an unpaired electron of mainly s character (i.e., $\bar{\mu}_n(s) = 1/n$ for n odd). In this way one would obtain for Fe_3 , for example, $\bar{\mu}_3 = 2.67\mu_B$ in better agreement with experiment and first-principles calculations.⁷ However, $\bar{\mu}_n(s)$ may be averaged out already at very low temperatures, since s - d exchange interactions are weak. Our calculations indicate that the variations in $\bar{\mu}_n$ as a function of n might be real since, as physically expected, $\bar{\mu}_n$ depends on bond length and geometrical arrangement of the atoms. s -electron contributions are known to be less structure sensitive. Therefore including them in the calculation should weaken the variation of $\bar{\mu}_n$. Additional correlations (beyond Hartree-Fock approximation) tend to yield saturated magnetic moments, and thus possibly reduce the variations of $\bar{\mu}_n$ for very small clusters. We conclude that in order to obtain reliable results for $\bar{\mu}_n$ it is necessary to determine more precisely correlations, the cluster structure, and the bond length without imposing any symmetry restrictions. For well-defined structures our results are in good agreement with experiment⁷ ($n=2,3$) and first-principles calculations^{8,9} ($n=9,15$). Therefore the theory presented here could be used to infer the structure of the clusters if precise experimental values for $\bar{\mu}_n$ were available.

B. Cr_n clusters

In order to obtain qualitative results for the equilibrium bond length and cohesive energy, we estimate the s -electron contribution to $E_{\text{coh}}(n)$ by adding to E_{band} the s -band energy contribution E_{band}^s . We consider an s -electron density of states of elliptical shape with size-dependent bandwidth W_i^s (i.e., second moment approximation³⁶), and neglect s - d hybridization effects and s - d charge transfer ($n_s=1$). For the s -electron hopping integrals we use a d^{-2} distance dependence¹⁹ yielding $W_i^s = (d_b/d)^2 (z_i^s/z_b^s)^{1/2} W_b^s$ (b refers to bulk and z_i^s to the effective s -electron coordination number).³⁶

Results for Cr_n clusters including the estimated s -electron contribution are given in Table IV. We see that the antiferromagnetic solution gives even for Cr_n ($n=2,3$) the largest cohesive energy, indicating that antiferromagnetic behavior of Cr bulk is already present for very small clusters. Upon relaxation most of the clusters contract, except ferro- Cr_2 , ferro- Cr_3 , and bcc- Cr_9 , for which an expansion is obtained (16% for ferro- Cr_2 , 21% for ferro- Cr_3 , and 1% for bcc- Cr_9). The expansion can be understood by noting that these clusters have very large local magnetic moments $\mu(i)$ which cause the repulsive magnetic force $F_{\text{mag}} = \partial(\Delta E_{\text{mag}})/\partial d$ [$F_{\text{mag}} \sim J \sum_i \mu(i) \partial \mu(i) / \partial d$] to be particularly large. To check

on the validity of this interpretation we calculated the relaxation for nonmagnetic [$\mu(i)=0$] bcc-Cr₉ and obtained a contraction of 2% in contrast to the magnetic one. Furthermore, for Cr₉ ΔE_{mag} is very large [$\Delta E_{\text{mag}}(9)=1.45$ eV] and thus F_{mag} dominates causing a small expansion. For Cr₁₅ the presence of the six second-nearest neighbors of the central atom causes $\mu(i)$ and thus ΔE_{mag} to reduce [$\Delta E_{\text{mag}}(15)=0.43$ eV], and the metallic bonding to increasing leading to a net attractive force at the bulk interatomic distance. For antiferromagnetic Cr₂ we obtain a much shorter bond length than for the bulk ($d_2/d_b=0.72$) in agreement with the contraction obtained in previous calculations.¹² In this case due to the antiferromagnetic order, the strong distance depen-

dence of the attractive d -electron bonding energy ($W_d \propto d^{-5}$) dominates. Note that relaxation does not change $\bar{\mu}_n$ for Cr _{n} ($n\bar{\mu}_n$ integer). However, due to the antiferromagnetic order the changes found in the local magnetic moments $\mu(i)$ are considerably large, since the hybridization between majority and minority orbitals of neighboring atoms changes.

Cr _{n} clusters with bcc-like structure ($9 \leq n \leq 51$) show antiferromagneticlike order with moments on atoms belonging to different sublattice of antiferromagnetic bulk-Cr pointing in opposite directions (e.g., Cr₉: $\uparrow\uparrow\uparrow$ and Cr₁₅: $\downarrow\uparrow\downarrow\uparrow\downarrow$). This is in agreement with results for Cr₉ and Cr₁₅ reported previously.¹⁰ Notice that for Cr₂₇ and Cr₅₁ $\mu(3)$ and $\mu(4)$ have the same sign (Cr₂₇: $\uparrow\uparrow\downarrow\uparrow\downarrow\uparrow\uparrow$

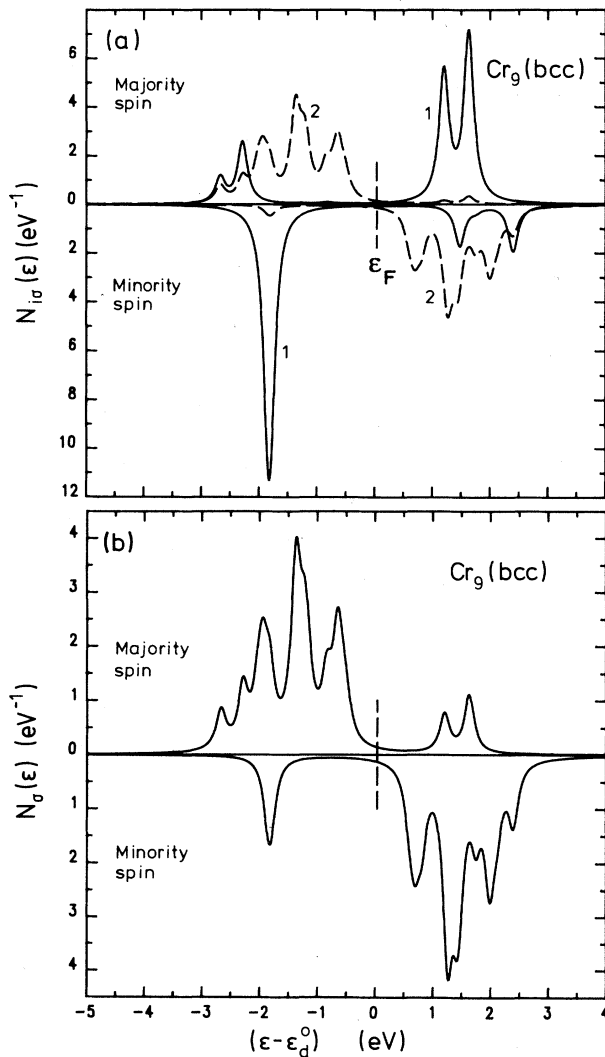


FIG. 5. (a) Local densities of states $N_{i\sigma}(\epsilon)$ and (b) average density of states $N_{\sigma}(\epsilon)$ of bcc-Cr₉, as in Fig. 2.

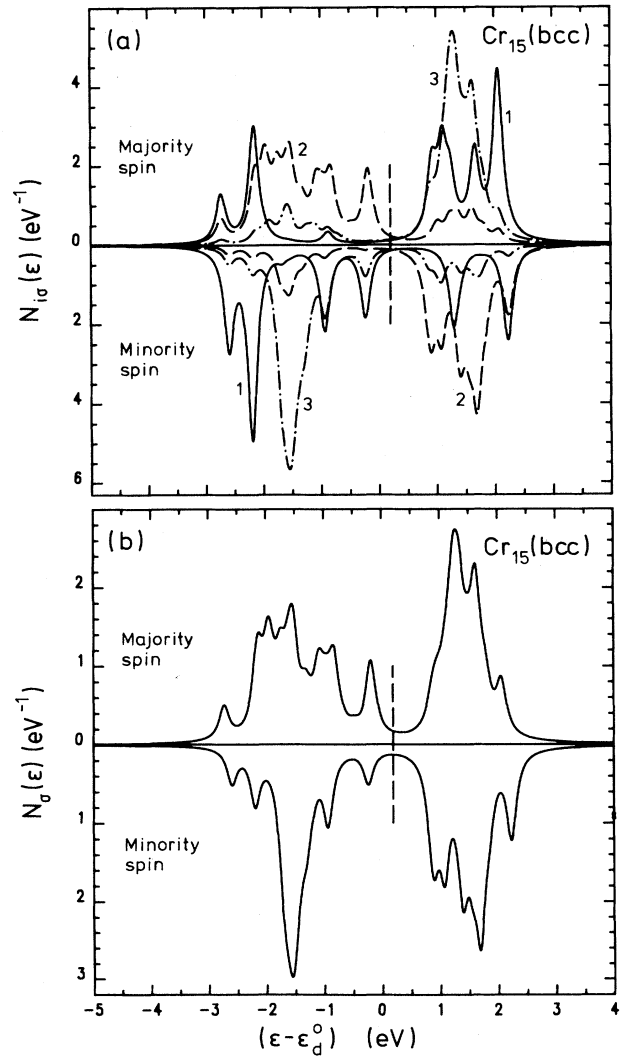
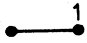
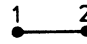

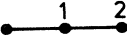





FIG. 6. (a) Local density of states $N_{i\sigma}(\epsilon)$ and (b) average density of states $N_{\sigma}(\epsilon)$ of bcc-Cr₁₅, as in Fig. 2.

TABLE IV. Results as in Tables II and III for Cr_n clusters.

	Structure	$E_{\text{coh}}(n)$	d_n/d_b	$\bar{\mu}_n$	$\mu(1)$	$\mu(2)$	$\mu(3)$	$\mu(4)$	$\mu(5)$
Cr_2		0.58 (0.36)	1.16	(5.00) (5.00)	5.00 (5.00)				
Cr_2		1.93 (0.89)	0.73	0.0 (0.0)	0.55 (4.60)	-0.55 (-4.60)			
Cr_3		0.75 (0.20)	1.21	5.00 (4.33)	5.00 (4.33)				
Cr_3		1.05 (0.99)	0.91	1.67 (1.67)	-3.54 (-4.32)	4.27 (4.66)			
Cr_4		0.88 (0.60)	0.96	0.50 (0.50)	0.50 (0.50)				
Cr_8		1.16 (0.98)	0.94	0.50 (0.50)	0.50 (0.50)				
Cr_8		0.78 (0.65)	0.96	2.25 (2.25)	2.25 (2.25)				
Cr_9	bcc	1.10 (1.09)	1.01	3.89 (3.89)	-2.71 (-2.71)	4.71 (4.71)			
Cr_{15}	bcc	1.79 (1.75)	0.98	0.33 (0.33)	-1.76 (-2.13)	2.90 (3.25)	-2.74 (-3.14)		
Cr_{27}	bcc	(1.64)		(1.96)	(1.89)	(-2.40)	(3.32)	(4.20)	
Cr_{51}	bcc	(2.02)		(1.24)	(-1.58)	(2.20)	(-2.11)	(-2.55)	(3.77)
Bulk	bcc	3.32	1.0	0.0	0.60	-0.60			

and Cr_{51} : $\uparrow\downarrow\downarrow\uparrow\downarrow\uparrow\downarrow\uparrow$). This is consistent, since atoms on these shells would belong to the same sublattice of antiferromagnetic bulk Cr (i.e., since they are second neighbors). The average magnetization $\bar{\mu}_n \rightarrow 0$ for increasing cluster size due to the cancellation of contributions with opposite sign. Already for Cr_{15} $\bar{\mu}_{15}$ is much smaller than the local magnetic moments, which at the surface of the cluster are remarkably large, even larger than those of Fe_n [$\bar{\mu}_{15} = 0.33\mu_B \ll |\mu(\text{surface})| \simeq 3\mu_B$]. Quantitatively our results for $\mu(i)$ of unrelaxed Cr_{15} disagree with those obtained by using the self-consistent $X\alpha$ approximation¹⁰ [$\mu_{X\alpha}(1) = -0.7$, $\mu_{X\alpha}(2) = 4.1$, and $\mu_{X\alpha}(3) = -3.4$]. This might be related to the particular treatment of exchange and correlation effects on which the results for antiferromagnetic Cr appear to depend sensitively.³⁷ However note that, as for Fe_n clusters, relaxation can cause appreciable changes in $\mu(i)$ which can be important when comparing with experiment.

In Figs. 5 and 6 the densities of states of Cr_9 and Cr_{15} are shown. Note that the typical antiferromagnetic-like shape with a deep valley at the center of the band near ϵ_F is already present for Cr_n ($n=9, 15$). For Cr_{15} we obtain a strong reduction of $N(\epsilon_F)$ and an increase of the width of the valley Δ_n with respect to bulk ($\Delta_{15} \simeq 1.2$ eV). For Cr_9 not only does $N(\epsilon_F)$ almost vanishes but also Δ_n increases ($\Delta_9 \simeq 2.2$ eV). This results would indicate a possi-

ble metal-insulator transition for small Cr_n clusters as a function of cluster size. However, further studies including explicitly s -electron and s - d hybridization effects and treating correlations beyond mean-field approximation are needed in order to draw definitive conclusions on this matter.

C. Ni_n clusters

Results for Ni_n are shown in Table V. As mentioned before, the magnetic moments of Ni_n clusters are larger than the bulk moment ($\mu_b = 0.6\mu_B$) in agreement with other calculations¹³ for Ni_{13} and Ni_{19} . In contrast to Fe_3 , we found that for Ni_3 the linear chain is slightly more stable than the triangular geometry, as obtained by other calculational procedures.³⁸ The magnetic energy gain ΔE_{mag} is larger for the linear chain ($\Delta E_{\text{mag}} = 0.03$ eV) than for the triangle ($\Delta E_{\text{mag}} = 0.01$ eV). This and the energy gained upon relaxation results in a larger binding energy for the linear chain and stabilizes this structure.

For Ni_n clusters with icosahedral-like and fcc-like structures ($13 \leq n \leq 43$) we obtain ferromagnetic-like order in contrast to fcc- or icosahedral- Fe_n . The calculated d -band width of fcc- Ni_{13} [$W_d(13) \simeq 4.3$ eV] agrees with first-principles calculations.¹² Furthermore our result for

$\bar{\mu}_n$ for fcc-Ni₁₉ ($\bar{\mu}_{19}=0.79\mu_B$) is in good agreement with LSDF calculations¹³ ($\bar{\mu}_{19}^{\text{LDA}}=0.80\mu_B$). For fcc-Ni₁₃ we obtain a larger average magnetic moment ($\bar{\mu}_{13}=0.85\mu_B$), but the value is somewhat smaller than the LSDF result¹³ ($\bar{\mu}_{13}^{\text{LDA}}=1.14\mu_B$). This is possibly due to $d \rightarrow s$ charge transfer (~ 0.2 electrons per atom) which might occur for very small clusters and which we have neglected by keeping constant the total number of d electrons n_d . Notice that the magnetic moments $\mu(i)$ of Ni _{n} ($n \leq 13$) with a nearly filled d band are particularly sensitive to the value of n_d since for these clusters the $\mu(i)$ are almost saturated [$\mu(i) \approx 10 - n_d(i)$]. In fact, for Ni₁₃ charge transfer from the central atom to the cluster surface, resulting mainly from the different effective bandwidth of the local density

of states of outer and inner atoms, causes $\mu(1)$ to be larger than $1.0\mu_B$ (see Table V). Magnetism and charge redistribution also play an important role in the structural stability of Ni clusters. In fact, if we set $U=0$ and $J=0$, and thus disregard effects due to magnetism and charge transfer, we obtain that icosahedral Ni₁₃ is more stable than fcc-Ni₁₃ ($E_{\text{coh}}^{\text{fcc}} - E_{\text{coh}}^{\text{icos}} = -0.07$ eV), in agreement with similar previous calculations.³⁹ If we take into account charge-transfer effects but still keep $J=0$, we obtain $E_{\text{coh}}^{\text{fcc}} - E_{\text{coh}}^{\text{icos}} = 0.02$ eV, indicating that fcc-Ni₁₃ is slightly favored. Now, using J as given in Table I, we obtain that fcc-Ni₁₃ is further stabilized by magnetism with respect to icosahedral Ni₁₃ ($E_{\text{coh}}^{\text{fcc}} - E_{\text{coh}}^{\text{icos}} = 0.06$ eV). This result illustrates the importance of calculating the spin-

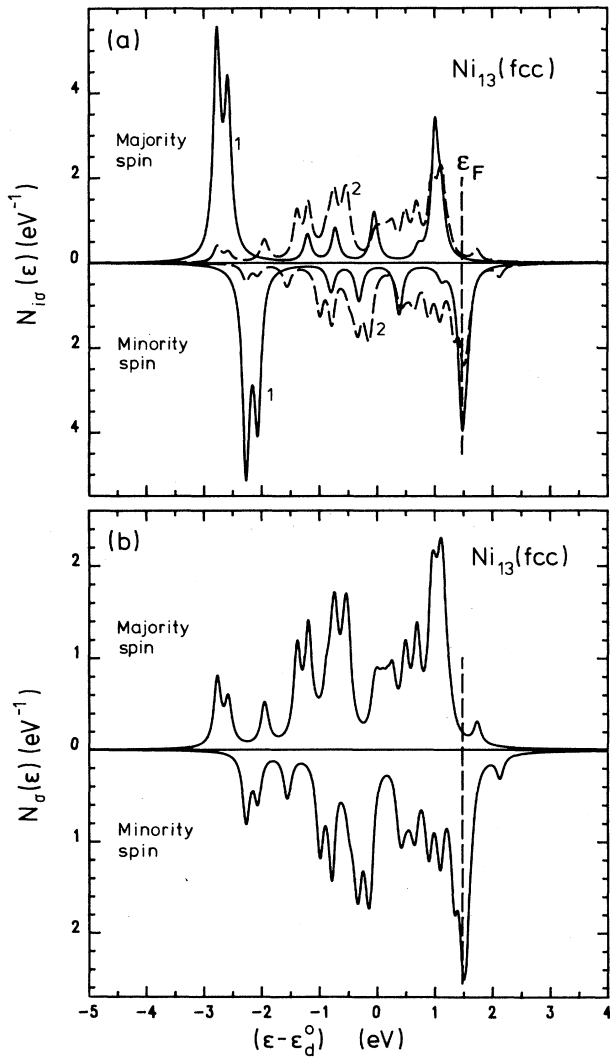


FIG. 7. (a) Local densities of states $N_{i\sigma}(\epsilon)$ and (b) average density of states $N_{\sigma}(\epsilon)$ of fcc-Ni₁₃ as in Fig. 2.

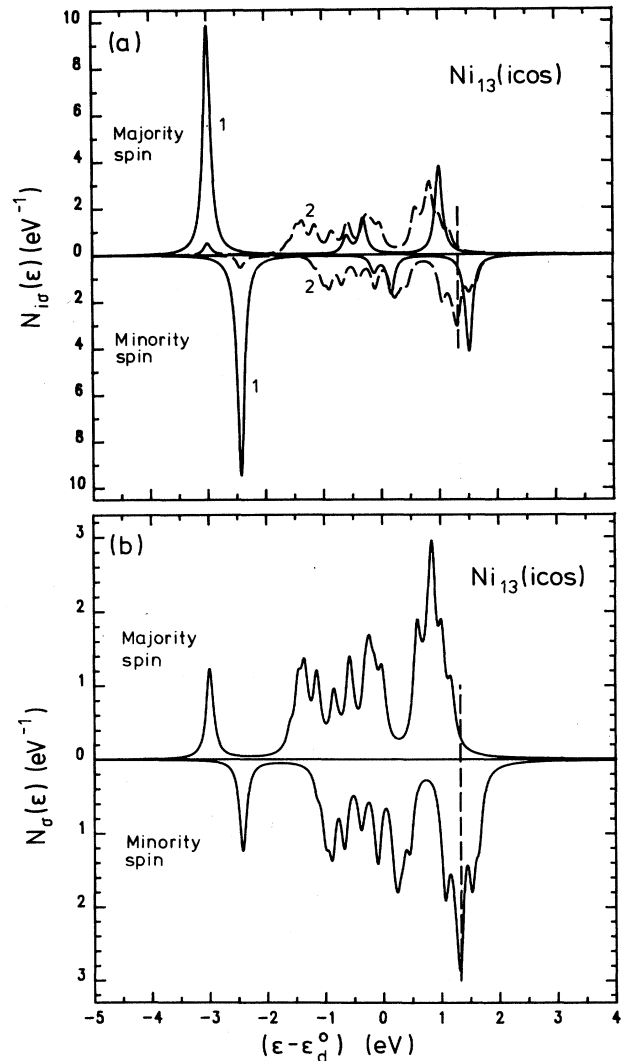
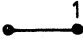

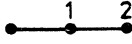





FIG. 8. (a) Local densities of states $N_{i\sigma}(\epsilon)$ and (b) average density of states $N_{\sigma}(\epsilon)$ of icosahedral-Ni₁₃ as in Fig. 2.

TABLE V. Results as in Tables II and III for Ni_n clusters. For Ni_{13} *a* refers to calculations using $U=4.5$ eV and $J=0$ (i.e., neglecting magnetic effects) and *b* to calculations using $U=0$ and $J=0$ (i.e., neglecting also charge-transfer effects). Otherwise the parameters listed in Table I were used.

	Structure	$E_{\text{coh}}(n)$	d_n/d_b	$\bar{\mu}_n$	$\mu(1)$	$\mu(2)$	$\mu(3)$	$\mu(4)$
Ni_2		0.66 (0.52)	0.92	1.00 (1.00)	1.00 (1.00)			
Ni_3		0.84 (0.68)	0.92	0.33 (0.33)	0.33 (0.33)			
Ni_3		0.87 (0.65)	0.90	0.33 (1.00)	0.33 (1.06)	0.33 (0.97)		
Ni_4		0.93 (0.81)	0.94	0.50 (0.50)	0.50 (0.50)			
Ni_8		0.98 (0.92)	0.96	0.75 (1.00)	0.75 (1.00)			
Ni_8		1.04 (0.93)	0.96	1.00 (1.00)	1.00 (1.00)			
Ni_{13}	fcc	1.07 (1.03)	0.97	0.85 (0.85)	1.28 (1.28)	0.81 (0.81)		
Ni_{13}	icos.	1.01 (0.93)	0.96	1.00 (1.00)	1.31 (1.31)	0.97 (0.97)		
Ni_{13}^a	fcc	0.99 (0.95)	0.97	0.0 (0.0)	0.0 (0.0)	0.0 (0.0)		
Ni_{13}^a	icos.	0.97 (0.85)	0.95	0.0 (0.0)	0.0 (0.0)	0.0 (0.0)		
Ni_{13}^b	fcc	1.15 (1.08)	0.97	0.0 (0.0)	0.0 (0.0)	0.0 (0.0)		
Ni_{13}^b	icos.	1.22 (1.09)	0.95	0.0 (0.0)	0.0 (0.0)	0.0 (0.0)		
Ni_{19}	fcc	1.09 (1.06)	0.99	0.79 (0.79)	1.07 (1.07)	0.79 (0.79)	0.74 (0.74)	
Ni_{43}	fcc	(1.15)		(0.72)	(0.88)	(0.80)	(0.70)	(0.67)
Bulk	fcc	1.18	1.0	0.6	0.6			

polarized charge distribution self-consistently, particularly when comparing structures with similar binding energies. However, we cannot conclude safely how the most stable geometrical arrangement of Ni_{13} should look like since the approximations we made (e.g., neglect of *s* electrons and *s-d* hybridization) preclude the determination of ΔE_{coh} to the accuracy required in this case (≈ 0.01 eV). Convergence to bulk behavior is almost reached for some properties of Ni_{43} . For example, the average magnetic moment $\bar{\mu}_{43}=0.72$ and cohesive energy $E_{\text{coh}}(43)=1.15$ eV are close to the bulk values $\mu_b=0.6\mu_B$ and $E_{\text{coh}}(b)=1.18$ eV.

In Figs. 7 and 8 we show results for the density of state of Ni_{13} with fcc- and icosahedral-like structure, respectively. Note that some of the main features of the fcc-bulk DOS are already present in fcc- Ni_{13} . For example,

$N_\sigma(\epsilon)$ shows a large peak near the top of the band, ϵ_F lies in the minority peak, and thus $N(\epsilon_F)$ is mainly of minority character. The shape of $N_\sigma(\epsilon)$ of fcc- and icosahedral- Ni_{13} are rather similar. However, some of the quantitative differences (e.g., the position of the peaks below ϵ_F) could be exploited to infer the cluster structure from future photoemission experiments.

IV. SUMMARY AND OUTLOOK

The size and structural dependence of magnetic properties of Cr_n , Fe_n , and Ni_n clusters were determined by using a tight-binding Hubbard Hamiltonian in the unrestricted Hartree-Fock approximation. The average magnetic moment $\bar{\mu}_n$, local magnetic moments $\mu(i)$, magnetic

ordering, cohesive energy, and average bond length were calculated at $T=0$. For all studied clusters we obtain larger magnetic moments than for bulk material. The increase of $\mu(i)$ becomes more important as we go from Ni to Cr, i.e., as we approach half-band filling, and Cr clusters show even larger magnetic moments than Fe clusters, in contrast to bulk material. Interesting dependence of the magnetic order within the cluster on structure and band filling has been obtained: bcc-Fe $_n$ is ferromagnetic-like whereas bcc-Cr $_n$ is antiferromagnetic-like, and fcc-Ni $_n$ is ferromagnetic-like whereas fcc-Fe $_n$ is antiferromagnetic-like. This behavior is related to the well-known increasing stability of the antiferromagnetic phase as we approach half-band filling.

The influence of magnetism on the structural stability was also studied. For example, we obtain that the energy due to magnetic and charge-transfer effects stabilizes the fcc structure with respect to the icosahedral structure for Ni $_{13}$, in contrast to previous calculations,³⁹ where these effects were neglected.

Our results for not too small clusters ($n \approx 15-19$) with unrelaxed symmetrical geometries are in good agreement with available first-principles calculations.⁸⁻¹³ Since the accuracy of the present theory should improve with increasing n , we expect to obtain reliable results also for larger clusters, which at present cannot be explored with first-principles methods. Furthermore, we can take into account geometric relaxation effects and no restrictions on the symmetry of the cluster are needed. This is particularly important since the most stable geometry of small clusters need not be of high symmetry.³⁵ Our calculations could be also easily extended to study chemisorption, vacancies, edge effects, etc., on clusters and surfaces.

Allowing uniform relaxation, the cluster interatomic distance d_n reduces typically⁴⁰ 2-4%. The variations of d_n versus n cause important changes in the size dependence of $\bar{\mu}_n$ which qualitatively improve the agreement with experimental results⁷ for Fe $_n$ ($n \leq 17$). However, note that in calculating the cluster-size dependence of the magnetic properties and cohesive energy we neglect for simplicity the s -electron contribution and s - d hybridization effects. These seem not to contribute much to the

size and structural dependence of the magnetic properties we calculate. However in some cases, s electrons can be important for determining bond length or structural changes. Thus, an indirect influence of the s electrons on the magnetic properties is expected and they should be taken explicitly into account in future calculations.

The temperature dependence of the magnetic properties of small clusters is of fundamental importance. In finite systems, the critical behavior is namely different from that in the bulk.⁴¹ Strong departures from bulklike behavior are expected to occur when the correlation length $\xi(T) \sim (T - T_c)^{-\gamma}$ becomes of the order of the cluster radius R . This is the case at temperatures $T \leq T^*$, where $(T^* - T_c) \sim R^{-1/\gamma}$. For example, the divergency at T_c in the specific heat $C_V(T)$ and magnetic susceptibility $\chi(T)$ disappears, since the long-wavelength magnetic fluctuations with wave-vector k ($k \rightarrow 0$) are naturally suppressed by the finite size of the cluster (i.e., $k \geq k_{\min} \sim 1/R$). Thus, rather than a divergency one obtains a peak with size-dependent width. Furthermore, it might be difficult to define a unique critical temperature $T_c(n)$ since the position of the peak in $C_V(T)$ and $\chi(T)$ can be different.⁴¹ In addition to the relevant temperatures $T^*(n)$ and $T_c(n)$, one is interested in the size dependence of the temperature $T_{SR}(n)$ at which short-range spin-spin correlations (e.g., between NN) are destroyed. We expect $T_{SR}(n)$ to be larger for small clusters than for the bulk since the magnetic moments $\mu(i)$ and thus the d -level exchange splitting $\Delta\epsilon_x = \epsilon_{d\downarrow} - \epsilon_{d\uparrow}$ and magnetic energy gain [$\Delta E_{\text{mag}} = E_{\text{band}}(\mu=0) - E_{\text{band}}(\mu)$] are larger. For clusters M_n with radius R smaller than the range of short-range spin order we expect spin alignment within the cluster ($n \lesssim 15$). It is difficult to draw definitive conclusions about the size dependence of $T_c(n)$. For small clusters one expects a reduced molecular field due to the reduced coordination number. If this dominates, then $T_c(n)$ should decrease with decreasing n . Clearly, reliable conclusions on the behavior of $T_c(n)$ must be based on an electronic theory, which takes into account the itinerant character of the d electrons. Extensions of our calculations to finite temperatures are currently in progress and will be published in due time.

*On leave of absence from Departamento de Física, Centro de Investigación de Estudios Avanzados del Instituto Politécnico Nacional (CINVESTAV-IPN), Apartado Postal 14-740, 07000 México, Distrito Federal, Mexico.

¹See, for instance, *Small Particles and Inorganic Clusters*, Proceedings of the 4th International Meeting on Small Particles and Inorganic Clusters, Aix-en-Provence, July 1988, edited by C. Chapon, M. F. Gillet, and C. R. Henry [Z. Phys. D. **12** (1989)].

²G. J. Johanson, M. B. McGirr, and D. A. Wheeler, Phys. Rev. B **1**, 3208 (1970); S. C. Abrahams, L. Guttman, and J. S. Kasper, Phys. Rev. **127**, 2052 (1962).

³J. Kübler, Phys. Lett. **81A**, 81 (1981).

⁴R. H. Victora, L. M. Falicov, and S. Ishida, Phys. Rev. B **30**, 3896 (1984).

⁵H. Hasegawa, J. Phys. F **16**, 347 (1986); J. Dorantes-Dávila, G. M. Pastor, and K. H. Bennemann, Solid State Commun. **60**, 465 (1986).

⁶H. Hasegawa and D. G. Pettifor, Phys. Rev. Lett. **50**, 130 (1983).

⁷D. M. Cox, D. J. Trevor, R. L. Whetten, E. A. Rohlfing, and A. Kaldor, Phys. Rev. B **32**, 7290 (1985).

⁸K. Lee, J. Callaway, and S. Dhar, Phys. Rev. B **30**, 1724 (1984).

⁹C. Y. Yang, K. H. Johnson, D. R. Salahub, J. Kaspar, and R. P. Messmer, Phys. Rev. B **24**, 5673 (1981).

¹⁰D. R. Salahub and R. P. Messmer, Surf. Sci. **106**, 415 (1981).

¹¹B. Delley, A. J. Freeman, and D. E. Ellis, Phys. Rev. Lett. **50**, 488 (1983).

¹²J. Bernholc and N. A. W. Holzwarth, Phys. Rev. Lett. **50**, 1451 (1983).

- ¹³K. Lee, J. Callaway, K. Kwong, R. Tang, and A. Ziegler, *Phys. Rev. B* **31**, 1796 (1985); R. P. Messmer, S. K. Knudson, K. H. Johnson, J. B. Diamond, and C. Y. Yang, *ibid.* **13**, 1396 (1976); H. Adachi, M. Tsukada, and C. Satoko, *J. Phys. Soc. Jpn.* **45**, 875 (1978); D. R. Salahub and F. Raatz, *Int. J. Quantum Chem.* **18**, 173 (1984).
- ¹⁴G. M. Pastor, J. Dorantes-Dávila, and K. H. Bennemann, *Physica B+C* **149B**, 22 (1988).
- ¹⁵G. M. Pastor, J. Dorantes-Dávila, and K. H. Bennemann, in *Physics and Chemistry of Small Clusters*, Vol. 158 of *NATO Advanced Study Institute, Series B: Physics*, edited by P. Jena, B. K. Rao, and S. N. Khanna (Plenum, New York, 1987), p. 463.
- ¹⁶Electron Correlation and Magnetism in Narrow-Band Systems, Vol. 29 of *Springer Series in Solid State Sciences*, edited by T. Moriya (Springer-Verlag, Berlin, 1981).
- ¹⁷O. K. Andersen, J. Madsen, U. K. Poulsen, O. Jepsen, and J. Kollár, *Physica B+C* **86-88B**, 249 (1977).
- ¹⁸R. Haydock, in *Solid State Physics* (Academic, London, 1980), Vol. 35, p. 215.
- ¹⁹V. L. Moruzzi and P. M. Marcus, *Phys. Rev. B* **38**, 1613 (1988); W. A. Harrison, *ibid.* **27**, 3592 (1983).
- ²⁰V. Heine, *Phys. Rev.* **153**, 673 (1967).
- ²¹J. L. Morán-López, K. H. Bennemann, and M. Avignon, *Phys. Rev. B* **23**, 5978 (1981).
- ²² $n_s \approx 1$ for $n > 2, 3$ seems reasonable due to maximal s bonding and $W_s \gg \epsilon_d - \epsilon_s$. Small s - d charge transfer does not qualitatively change our results.
- ²³V.L. Moruzzi, J. F. Janak, and A. R. Williams, in *Calculated Electronic Properties of Metals* (Pergamon, New York, 1978).
- ²⁴A first check on the accuracy of the model and parameter choice is provided by the d -level exchange splitting $\Delta\epsilon_x = \epsilon_{d\downarrow} - \epsilon_{d\uparrow}$ calculated for bulk material. We obtain $\Delta\epsilon_x(\text{Cr}) = 0.34$ eV, $\Delta\epsilon_x(\text{Fe}) = 1.61$ eV, and $\Delta\epsilon_x(\text{Ni}) = 0.30$ eV in good agreement with experimental findings and previous calculations (Ref. 25): $\Delta\epsilon_x(\text{Cr}) \approx 0.4$ eV, $\Delta\epsilon_x(\text{Fe}) = 1.3-2.2$ eV, and $\Delta\epsilon_x(\text{Ni}) = 0.3-0.6$ eV.
- ²⁵L. W. Bos and D. W. Lynch, *Phys. Rev. B* **2**, 4567 (1970); J. Callaway and C. S. Wang, *ibid.* **16**, 2095 (1977); **15**, 298 (1977).
- ²⁶V. Heine, in *Solid State Physics* (Academic, London, 1980), Vol. 35, p. 1.
- ²⁷Similar conclusions can be inferred from the success of tight-binding calculations for transition-metal surfaces (see Ref. 4).
- ²⁸Note that the magnetic moments $\mu(i)$ are rather insensitive to s - d hybridization effects since they are given by an integral over the DOS, and thus are somewhat independent of the details in the d -level energy distribution.
- ²⁹Note that the discrete cluster energy levels were broadened using a Lorentzian of width $\gamma = 0.2$ eV. This value was chosen in order to compare with the results of Refs. 8 and 9.
- ³⁰J. Callaway and C. S. Wang, *Phys. Rev. B* **16**, 2095 (1977).
- ³¹A similar slow convergence of the local magnetic moments $\mu(i)$ to the corresponding bulk value has been obtained near surfaces of transition metals. Here even at the fourth layer below the surface, deviations from the bulk value were found [H. Hasegawa, *J. Phys. F* **16**, 1555 (1986); **16**, 347 (1986)].
- ³²W. Keune, R. Halbauer, U. Gonser, J. Lauer, and D. L. Williams, *J. Magn. Magn. Mater.* **6**, 192 (1977); U. Gonser, (private communication).
- ³³G. M. Pastor, J. Dorantes-Dávila, and K. H. Bennemann, *Chem. Phys. Lett.* **148**, 459 (1988).
- ³⁴D. G. Pettifor, *J. Phys. C* **3**, 367 (1970).
- ³⁵Note that *ab initio* results for alkali-metal clusters (e.g., Li_n , $n \leq 13$) suggest that rather low-symmetry clusters may be more stable than high-symmetry ones. M. H. McAdon and W. A. Goddard, *Phys. Rev. Lett.* **23**, 2563 (1985); *J. Chem. Phys.* **88**, 277 (1988); V. Bonačić-Koutecký, P. Fantucci, and J. Koutecký, *Phys. Rev. B* **37**, 4369 (1988).
- ³⁶D. Tománek, S. Mukherjee, and K. H. Bennemann, *Phys. Rev. B* **28**, 665 (1983).
- ³⁷J. Chen, D. Singh, and H. Krakauer, *Phys. Rev. B* **38**, 12834 (1988).
- ³⁸A. B. Anderson, *J. Chem. Phys.* **64**, 4046 (1976); **66**, 5108 (1977); H. Basch, M. D. Newton, and J. W. Moskowitz, *ibid.* **73**, 4492 (1980).
- ³⁹M. B. Gordon, F. Cyrot-Lackmann, and M. C. Desjonquères, *Surf. Sci.* **80**, 159 (1979).
- ⁴⁰However, bcc-like Cr_9 shows a 1% expansion, which results mainly from the increased repulsive magnetic force [$F_{\text{mag}} \sim J \sum_i \mu(i) \partial \mu(i) / \partial d$] associated with the formation of local magnetic moments, which in Cr_9 are exceptionally large.
- ⁴¹P. G. Watson, in *Phase Transitions and Critical Phenomena*, edited by C. Domb and M. S. Green (Academic, London, 1972), Vol. 2, p. 101; M. N. Barber, in *Phase Transitions and Critical Phenomena*, edited by C. Domb and J. L. Lebowitz (Academic, London, 1983), Vol. 8, p. 145.